Sub micro liter Electrochemical Single-Nucleotide-Polymorphism Detector for Lab-on-Chip System

Hiroyuki Tanaka[1, 2*], Paolo Fiorini[2], Sara Peeters[2], Bivragh Majeed[2], Tom Sterken[2], Maaike Op de Beeck[2], Miho Hayashi[3], Hidenobu Yaku[1, 4], and Ichiro Yamashita[1]

[1] Advanced Technology Research Laboratory, Panasonic Corporation.
Seika, Kyoto 619-0237, Japan

[2] IMEC vwz., Kapeldreef 75, B-3001 Leuven, Belgium

[3] R&D Center, Panasonic Healthcare Corporation.
Toon, Ehime 791-0395, Japan

[4] Frontier Institute for Biomolecular Engineering Research (FIBER), Konan University,
Kobe 650-0047, Japan

[*] E-mail address: tanaka.hiroyuk@jp.panasonic.com

A sub-micro-liter single-nucleotide-polymorphism (SNP) detector for lab-on-chip applications is developed. This detector enables a fast, sensitive, and selective SNP detection directly from human blood. The detector is fabricated on a Si substrate by a standard complementary metal oxide semiconductor / micro electro mechanical systems (CMOS/MEMS) process and Polydimethylsiloxane (PDMS) molding. Stable and reproducible measurements are obtained by implementing an on-chip Ag/AgCl electrode and encapsulating the detector. The detector senses the presence of SNPs by measuring the concentration of pyrophosphoric acid generated during selective DNA amplification. A 0.5-μL-volume detector enabled the successful performance of the typing of a SNP within the ABO gene using human blood. The measured sensitivity is 566

pA/μM.

1. Introduction

A single nucleotide polymorphism (SNP) is a single nucleotide variation from the DNA consensus sequence that can result in differences between people's reaction to pathogens, chemicals, drugs, etc. Hence, SNP genotyping has shown increasing importance in medical health care.[1, 2] However, SNP detection methods currently used for bio medical check require large dedicated equipment, large amounts of samples, and an extensive sample preparation. Furthermore, some methods have issues of limited SNP specificity and sensitivity .[3] The integration of microfluidic components and SNP detectors with high sensitivity on a small die, i.e., a lab-on-a-chip (LoC) device, is expected to resolve these present issues.

Recently, LoC technology has been making remarkable progress. The miniaturization of the microfluidic system and analysis sensor brought many merits, i.e., fast analysis, small void volume, low power consumption, multi-parallel detection capability, and low cost. In particular, the considerably large reduction in sample and reagent volumes is beneficial for shorter turnaround time and lower cost.[4-6]. This LoC technology is now applied to DNA analysis. The use of LoC having polymerase chain reaction (PCR) and the subsequent DNA analysis have made great success and some products are ready for commercialization.[7-10] Cho *et al.* reported a microfluidic LoC having a micro-PCR fabricated on a silicon substrate by MEMS process technology for the rapid detection of the hepatitis B virus,[7] and Palmieri *et al.* investigated a LoC comprising a micro-PCR device.[8] However, there are only a few reports on LoC systems where PCR is coupled to SNP detection. [10]

A variety of detection approaches have been explored for SNP detectors.[11-15] Among them, electrochemical SNP detection methods have been attracting researchers' attention owing to

their excellent features such as high sensitivity, low cost, ease of miniaturization, and portability.[13] However, the methods have a drawback, which is the issue of false positive signals False positive signals arise from the nonspecific binding of redox reporters[16] or from the low sensitivity caused by limited probe-DNA immobilization and hybridization on the electrode. In our previous work, [17, 18] we reported an electrochemical detector employing a novel allele-specific primer (ASP) that initiates PCR amplification only in presence of a SNP. The detector could detect pyrophosphoric acids produced by PCR operation when a SNP exists. The detection was in an all-or-nothing manner, which excluded false positive signals. Using a sample volume of 20 μL, accurate allele detection was demonstrated manually. However, to implement the SNP detector in the LoC, considerable size reduction is needed, which inevitably decreases the signal amplitude significantly. Even more, a very small volume of sample is susceptible to evaporation during PCR operation.

Our previous work, we designed a small LoC system with electrochemical SNP detector so as to enables fast SNP detection directly from blood with high sensitivity and specificity suited for point of care applications.[19] Figure 1 shows the operation principle and a schematic drawing of the LoC. Most of the components are fabricated on a Si substrate using CMOS/MEMS processing techniques.[20] Pumps,[21] valves, and detectors are fabricated separately and later embedded in or on the chip. Through DNA extraction, amplification, purification, and separation, DNA fragments with the SNP region of interest are isolated and routed to the SNP detectors. The LoC system can detect multiple SNPs simultaneously (one for each implemented detector).

In this paper, we report a newly designed Si based SNP detector that could be implemented in our previously reported LoC system. The detector has an appropriately encapsulated chamber with a large electrode area to ensure sufficient charge transfer from reactants at the electrode

surface and has an integrated reference Ag/AgCl electrode. Severe evaporation was minimized by appropriate encapsulation. The typing of a SNP within the ABO gene using human blood was also demonstrated using the newly designed detector.

2. Detector Fabrication, Operating Principle, and Experimental Procedure

2.1 Detector fabrication

The detector chip is composed of three electrodes [counter electrode, reference electrode and working electrode, see Fig. 2(a)], placed in a cavity. It was fabricated on a Si wafer by a standard CMOS/MEMS fabrication technique. Prior to electrode formation, a silicon-nitride layer with thickness of 100 nm was deposited on the silicon surface by plasma enhanced chemical vapor deposition (PECVD); this layer is necessary for electrical isolation between electrodes. Then, the electrodes were defined by a lift-off process; they were fabricated from a 100-nm-thick gold layer deposited on a 5-nm-thick titanium adhesion layer. The working electrode area is 0.29 mm^2. Circular cavities were formed by PDMS molding and perfectly aligned to the electrode patterns. The cavity diameter is 1.8 mm and the thickness of PDMS is 300 μm; this gives a detector volume of 0.5 μL. Beside this measurement cavity, a second smaller cavity, connected to it, was formed [see Fig. 2(a)]. It is used for sample loading and for accessing the reference electrode. After forming the cavities, part of the reference electrode was covered with AgCl/Ag ink commercialized by ALS. Finally, the detector was covered by a polymer cover plate to prevent the evaporation of the sub micro liter solution during the measurement. The plate has a very small aperture towards ambient to allow air evacuation during the filling pro-

cedure. The fabricated chip is shown in Fig. 2(b).

2.2 SNP detection principle

The operation of the SNP detector involves two steps. The first step is the specific DNA replication using an ASP. The second step is pyrophosphoric acid (PPi) detection using an electrochemical method. Specific DNA replication is described on top of Fig. 3. The SNP is identified by a smartly designed ASP having one complementary base corresponding to the SNP base and two non complementary bases at the 3' end. Owing to the use of this ASP, elongation and amplification during PCR are only initiated when the SNP is present.

The detailed electrochemical detection is described in ref. 18, which is schematically drawn at the bottom of Fig. 3. One PPi molecule is produced for each deoxyribonucleotide triphosphate (dNTP) incorporation during amplification. Therefore, the concentration of PPi will be detected only in presence of a SNP.

PPi is detected through a cascade of chemical reactions involving three catalyst enzymes: pyrophosphatase, glyceraldehyde-3-phosphate dehydrogenase (GAPDH), and diaphorase.

First, PPi is hydrolyzed to phosphoric acid (Pi) in the presence of pyrophosphatase:

$$PPi + H_2O \Leftrightarrow 2Pi. \quad (1)$$

Then, the obtained Pi is mixed together with glyceraldehyde-3-phosphate (GAP), and nicotinamide adenine dinucleotide (NAD^+). In the presence of GADPH, the following reaction takes place:

$$Pi + GAP + NAD^+ \Leftrightarrow \text{1,3-bisphosphoglyceric acid} + NADH. \quad (2)$$

Next, NADH is mixed with potassium ferricyanide ($K_3[Fe(CN)_6]$), which, in the presence of diaphorase, is converted into potassium ferrocyanide $K_4[Fe(CN)_6]$ according to the follow-

ing reaction:

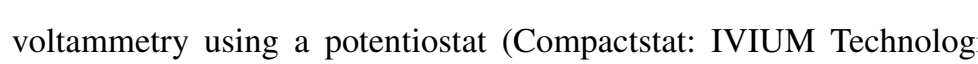

$$NADH + H^+ + K_3[Fe(CN)_6] <=> NAD^+ + K_4[Fe(CN)_6]. \quad (3)$$

Finally, the $[Fe(CN)_6]^{4-}$ ion is detected electrochemically: at the detector electrode, it is oxidized back to ferricyanide $[Fe(CN)_6]^{3-}$, and then electrons are released and current flows in the detector circuit.

2.3 Measurement procedure

2.3.1 Measurements with ferricyanide for detector optimization

Cyclic voltammetry using a potentiostat (Compactstat: IVIUM Technologies B.V, Netherland) was used to determine the working potential window and the corresponding current variation. A 0.4 mM solution of $K_3[Fe(CN)_6]$ in 0.1 M KCl solution was used . The concentration of $K_4[Fe(CN)_6]$ is similar to the typical concentration under real operation conditions. The potential of the working electrode was scanned from −0.6 to 0.8 V at a scan rate of 100 mV per second. The voltage scan was repeated 5 times to observe the variation in current.

2.3.2 Measurement with PPi for detector characterization

PPi detection was demonstrated at a concentration typical for SNP DNA replication. The same potentiostat was used in a chronoamperometric mode. Four different concentrations of PPi (0, 0.1, 0.3, and 1 mM) were prepared in 45 mM tricine-NaOH buffer (pH 8.5) containing GAP (10 mM), NAD^+ (1 mM), $K_3[Fe(CN)_6]$ (10 mM), $MgCl_2$ (1.7 mM), diaphorase (10 U/mL), GAPDH (32 U/mL), and pyrophosphase (5 U/mL). After preparing 20 μL of the mixture, only

0.5 μL was transferred to the cavity of the detector chip. The potential of the working electrode was set at 0.6 V and the time dependence of the current was measured; the measurement was repeated five times for each of the PPi mixtures.

2.3.3 SNP typing

In this work, SNP detection was demonstrated in the ABO gene. Exon 6 of this gene contains a SNP at the 22nd base pair, which is used for human blood genotyping. This base pair is a G/C base pair in the A and B alleles and an A/T base pair in the O allele.[22, 23)] This change is due to the deletion of the G/C base pair in the A and B alleles. In our experiments we used AB and O blood samples. A two-step PCR reaction was carried out to detect the SNP. In the 1st PCR reaction, the fragment containing the SNP was selected and enriched using the following primers: forward primer (5'-TAGGAAGGATGTCCTCG-3') and reverse primer (5'-TTCTTGATGGCAAACACAGTTAAC-3') (Life Technologies, custom DNA oligonucleotides). The first PCR was carried out in a 10 μL tube, using 0.2 mM dNTP, 0.02 U/μl KOD polymerase purchased from Toyobo Bio Technology, Co., Ltd., 0.5 μM each of the forward and reverse primers, and 1.8 μL of the template (blood) in 5 μL of buffer solution for KOD polymerase. A negative control sample (NTC) was also prepared by adding water instead of blood. Following denaturation at 95 ^{o}C for 4 min, 35 cycles of denaturation at 95 ^{o}C for 30 s, annealing at 60 ^{o}C for 30 s, and extension at 72 ^{o}C for 30 s were carried out. Then, the amplicons obtained from 1st PCR were centrifuged to separate the supernatant containing the extracted DNA fragments from the mixture including some jelly parts. Next, the separated supernatant was diluted 1000 times in water to reduce the concentration of PPi produced during the 1st PCR. This dilu-

tion is necessary because a large PPi concentration causes a large background signal and a low signal/noise ratio.

To detect the SNP using allele-specific primers, a 2nd PCR was carried out using the diluted product of the 1st PCR as the template and the allele-specific forward primer: 5' -TAGGAAGGATGTCCTCGTGACG-3'. The reverse primer was the same as that used in the first PCR.The 10 μL PCR mixtures contained 0.02 U/μL platinum Taq polymerase (supplied by Invitrogen), 1.5 μL of PCR buffer for platinum Taq containing dNTP, 1 μM each of the forward and reverse primers, and 2 μL of the template. Following DNA denaturation at 95 ^{o}C for 10 min, the 2nd PCR was carried out for 18 cycles identically to the 1st PCR. After that, the resulting PCR amplicons were mixed with the same solution used for PPi detection. Finally, 0.5 μL each of these mixtures was added to the electrochemical detector. Detection was again performed by setting the potential of the working electrode at 0.6 V and measuring the time dependence of current. The measurement was repeated five times for each sample.

3. Results and Discussion

3.1 Detector structure optimization

In a previous paper,[19)] it was demonstrated the electrochemical detector with a cavity depth of 300 μm and a volume of 0.5 μL could have the required sensitivity. However, for the detector, current spikes were observed during the measurement from time to time. The spikes were attributed to the open detector cavity configuration with a simply immersed reference Ag/AgCl wire electrode. Since a patterned gold electrode could not be used as the reference electrode, the

Ag/AgCl wire was simply immersed in the solution. In some occasions, the reference Ag/AgCl wire vibrated in the fluid causing the current spikes.

In the prototype SNP detector presented here, the stability problem was solved by integrating a Ag/AgCl electrode. The previous Ag/AgCl wire was replaced with a gold-patterned electrode covered with Ag/AgCl ink. The Ag/AgCl ink was stable enough against the sample solution during the measurement period. Figure 4(a) shows five consecutive cyclic voltammetry measurements performed in an open cavity detector having an on-chip Ag/AgCl reference electrode. Measurements were performed following the procedure described in §2.3.1. Well-defined and regular redox current loops were observed and no current peaks were observed. The peak currents, at which the oxidation of ferricyanide to ferrocyanide starts, were observed at approximately 0.4 V.

It was notable that the absolute current value was increased as measurement cycle increased. For example, the current measured at 0.6 V increased by 14% from the first to the fifth cycle. This large variation could result in the poor reproducibility of the SNP detection process. We speculated that this effect was due to the evaporation of the solution. The cavity was covered with a polymer plate to suppress the evaporation for stability improvement. Figure 4(b) shows the results of five cyclic-voltammetory measurements with the encapsulated structure. The cyclic-voltammetry loop traced the almost the same trajectories. The current drift at a voltage of 0.6 V was reduced from 14 to 3.5%. [Fig. 4(c)]. The values reported in Fig. 4(c) were stable against the typical temperature variations of our laboratory (19-22 ^{o}C). No detailed investigation of the effect of temperature in a wider range has been performed.

3.2 PPi detection

To characterize the sensitivity of our SNP detector, PPi mixtures with various concentrations were measured. As mentioned above, one molecule of PPi is produced for one-base elongation during DNA replication according to the following equation (4):

$$\text{DNA (n)} + \text{dNTP} \Longleftrightarrow \text{DNA (n+1)} + \text{PPi}. \tag{4}$$

where dNTP represents a generic nucleotide. The concentration of PPi produced in this reaction is equal to that of DNA multiplied by the number of base pairs contained in the DNA strand. During PCR, the accumulation of DNA slows down when its concentration reaches approximately 100 nM,[24] and the final concentration is at most ~1 μM. In our LoC system, the DNA strands have typical length of 100-150 bp; thus, PPi concentration should be in the 0.1-0.3 mM range. Therefore, the concentrations of PPi in the mixture were prepared as 0, 0.1, 0.3, and 1 mM and used for the PPi detection check.

Figure 5(a) shows the time dependence of the current vs. PPi concentration with a voltage of 0.6 V. Each curve is an average of five measurements. At all concentrations, the current first decreases steeply. A slower decrease followed until the current became constant. The results could be interpreted as follows. Just after bias application, the ion concentration near the electrode is high. Highly concentrated ions were oxidized and generated a large current. With the depletion of ions in the region near the electrode, the current gradually decreased. At equilibrium, a stationary ion gradient is established and the current was governed by the ion diffusion coefficient.

It is clear that measuring the rapidly varying current just after the bias application might generate large errors. For this reason, we always measured the detector current 30 s after bias application. Figure 5(b) shows the average current and its variation (shown in error bar) at 30 s

vs the PPi concentration. The current is proportional to the PPi concentration up to 0.3 mM, which corresponds to the typical PPi concentration after DNA replication. However, the current for 1 mM is about twice smaller than expected. This behavior is due to the depletion of the NAD reactant. As indicated by eqs. (1) and (2), four molecules of NAD are necessary for the detection of one molecule of PPi. In other words, we need 2 mM NAD if we want to detect 1 mM PPi. Since there is only 1 mM NAD in the used reaction mixture the signal is reduced by a factor of two. Therefore, we conclude that the detection signal is proportional to the PPi concentration up to 0.5 mM. Obviously, this range can be easily varied by changing the NAD concentration.

In the explored range, the sensitivity is 566 pA/μM which is comparable to a value of 1000 pA/μM reported in ref. 20 for a detector with a 3.3 times larger electrode area. The results presented in this paper indicated that the newly designed detector has good sensitivity sufficient for SNP detection.

3.3 SNP typing

The detection procedure is shown in Fig. 6. In a first step, the DNA fragment exon 6 of the ABO gene was selected and amplified by a 1st PCR following the procedure described in §2.3.3. The lysis of white blood cells was performed in the same PCR cavity by a 10 min heating step at 95 ^{o}C. Figure 7 shows the electrophoresis patterns after the first PCR. In lanes 2 and 3, clear bands are observed, which indicates that the selected DNA fragments of 135 and 134 bp from the AB and O blood samples, respectively were successfully amplified, whereas, in lane 4, there was no amplification for the negative control (NTC) fragment prepared by replacing blood

with pure water.

After that, a second allele-specific PCR (2nd PCR) was conducted as described in §2.3.3. The selectivity of 2nd PCR with respect to SNP presence was confirmed by gel electrophoresis as indicated by lanes 6 and 7 in Fig 7. Only the AB fragment is amplified (lane 6), while the O fragment (lane 7) and NTC (lane 8) are not.

Finally, AB and O blood typing was carried out using the SNP detector. The amplicon obtained after the 2nd PCR is added to the mixture, which was used for PPi detection. The percent in volume of the amplicon in this experiment is equal to the percent in volume of PPi in the experiments described in the previous section. Figure 8(a) shows the time dependence of the average current with the amplicon from AB and O blood samples, and with the NTC sample. The current from the AB amplicon was always larger than that from the O amplicon and NTC. Figure 8(b) shows the net signals, which are the differences of the AB signal minus the NTC signal and of the O signal minus the NTC signal. A clear difference between the AB and O amplicons is observed. Experiments have been repeated five times for each sample, and the measured fluctuation of the signal, which is shown by error bar, is quite small, as shown in Fig. 8(b). The efficiency of the SNP detector was demonstrated.

4. Conclusions

We presented an electrochemical SNP detector with a 0.5 μL volume and appropriate cavity/electrode structure and that operates by encapsulation. PPi detection and also SNP detection in the ABO gene from blood are successfully demonstrated in the improved structure. These results enable the realization of a small and portable LoC SNP detection system, which

will perform a fast and simultaneous detection of multiple SNPs.

Acknowledgments

The authors would like to thank Dr. C. Van Hoof at IMEC for his helpful support and encouragement throughout this work. The authors also would like to thank Dr. M. Hiraoka for many discussions throughout this work.

1) N. J. Schork, D. Fallin, and J. S. Lanchbury: Clin. Genet. **58** (2000) 250.

2) J. J. McCarthy and R. Hilfiker: Nat. Biotechnol. **18** (2000) 505.

3) R. Rapley, and S. Harbron: *Molecular Analysis and Genome Discovery* (Wiley, Chichester, U.K. 2004)

4) J. Kian-Kok Ng, and W.-T. Liu: Anal. Bioanal. Chem. **386** (2006) 427.

5) P. R. Selvaganapathy, E. T. Carlen, and C. H. Mastrangelo: Proc. IEEE **91** (2003) 954.

6) F. Vinet, P. Chaton, and Y. Fouillet: Microelectron. Eng. **61** (2002) 41.

7) Y.-K. Cho, J. Kim, Y. Lee, Y.-A. Kim, K. Namkoong, H. Lim, Kwang W. Oh, S. Kim, J. Han, C. Park, Y. E. Pak, C. Ko, C.-S. Ki, J. R. Choi, and H.-K. Myeong: Biosens. Bioelectron., **21** (2006) 2161.

8) M. Palmieri, T. Barbuzzi, A. Maierna, M. Marchi, G. Montalbano, G. Panvini, T. Rodenfels, and W. Stoeters: Ext. Abstr. 43rd Int. Symp. Microelectronics (IMAPS2010), 2010, p. 36.

9) S. L. Marasso, E. Giuri, G. Canavese, R. Castagna, M. Quaglio, I. Ferrante, D. Perrone, and M. Cocuzza: Biomed. Microdevices **13** (2011) 19.

10) J.Y. Choi, S. J. Choi, Y. Chen, H. W. Kim, S. A. You, H.-K. Myeong, and T.S. Seo: Ext. Abstr. 14th Int. Conf. Miniaturized Systems for Chemistry and Life Sciences (μ-TAS2010), 2010, p. 136.

11) B. W. Kirk, M Feinsod, R. Favis, R. M. Kliman, and F. Barany: Nucleic Acid Res. **30** (2002) 3295.

12) S, Tyagi, and F. R. Kramer: Nat. Biotechnol. **14** (1996) 303.

13) I. Willner: Science **298** (2002) 2407.

14) Y. Akagi, M. Makimura, Y. Yokoyama, M. Fukazawa, S. Fujiki, M. Kadosaki, and K. Tanino: Electrochim. Acta **51** (2006) 6367.

15) J. Wakai, A. Takagi, M. Nakayama, T. Miya, T. Miyahara, T. Iwanaga, S. Takenaka, Y. Ikeda, and M. Amano: Nucleic Acids Res. **32** (2004) e141.

16) Y. Xiao, X. Lou, T. Uzawa, K. J. I. Plakos, K. W. Plaxco, and H. T. Soh: J. Am. Chem. Soc. **131** (2009) 15311.

17) H. Yaku, T. Yukimasa, T. Nakao, S. Sugimono, and H. Oka: Electrophoresis, **29** (2008) 4130.

18) H. Yaku, T. Yukimasa, and H. Oka: Panasonic Tech. J., **54**-2 (2008) 40 [in Japanese].

19) M. Op de Beeck, W. De Malsche, M. Hiraoka, P. Fiorini, L. Zhang, J. Op de Beeck, B. Majeed, H. Tanaka, D. S. Tezcan, G. Desmet, D. Ueda, C. Van Hoof, and I. Yamashita: IEDM Tech. Dig., 2010, p. 824.

20) B. Majeed, B. Jones, D. S. Tezcan, N. Tutunjyan, L. Haspeslagh, S. Peeters, P. Fiorini, M. Op de Beeck, C. Van Hoof, M. Hiraoka, H. Tanaka, and I. Yamashita: submitted to Jpn. J. Appl. Phys.

21) M. Hiraoka, P. Fiorini, J. O'Callaghan, I. Yamashita, C. Van Hoof, M.O. Beeck: to be published in Sens. Actuators, A (2011), [DOI: 10.1016/j.sna.2011.08.024].

22) F. Yamamoto, and S. Hakomori: J. Biol. Chem. **264** (1990) 19257.

23) F.Yamamoto, H. Clausen, T. White, J. Marken, and S. Hakomori: Nature **345** (1990) 229.

24) J. M. Butler: *Fundamentals of Forensic DNA Typing* (Academic Press, New York 1969) p. 120.

Figure captions:

Fig. 1: (Color online) Functional blocks of SNP detection system and its schematic cross section.

Fig. 2: (Color online) (a) Schematic view of SNP micro detector. (b) Photograph of the fabricated chip.

Fig. 3: (Color online) SNP detection flow based on allele specific primer (ASP) and electrochemical reaction. See text for explanation.

Fig. 4: (Color online) (a) Cyclic voltammetry curves measured without encapsulation. Four measurements are performed one after the other to visualize drift. (b) Same measurements in an encapsulated cavity . (c) Current variations in open and encapsulated cavities.

Fig. 5: (Color online) (a) Current vs time for different concentrations of PPi (0, 0.1, 0.3, and 1 mM).

(b) Current at t=30 s vs PPi concentration. Increase and saturation of current are indicated by dotted lines.

Fig. 6: (Color online) Detection flow of SNP in exon 6 of ABO gene.

Fig. 7: (Color online) Gel electrophoresis results in ABO gene from AB and O type blood samples.

Fig. 8: (Color online) SNP detection results in ABO gene from AB and O type blood samples.

(a) Current vs. time for AB, O, and negative control (NTC) after amplification using ASP.

(b) Currents at t=30 s for AB and O fragments after baseline (for NTC) subtraction.

Fig. 1

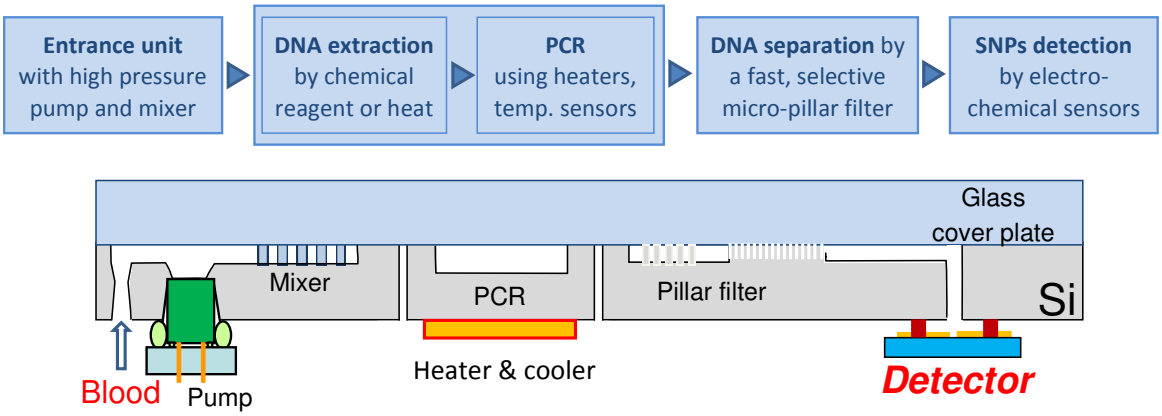
Entrance unit with high pressure pump and mixer
DNA extraction by chemical reagent or heat
PCR using heaters, temp. sensors
DNA separation by a fast, selective micro-pillar filter
SNPs detection by electro-chemical sensors
Glass cover plate
Mixer
PCR
Pillar filter
Si
Blood
Pump
Heater & cooler
Detector

Fig. 2

(a)

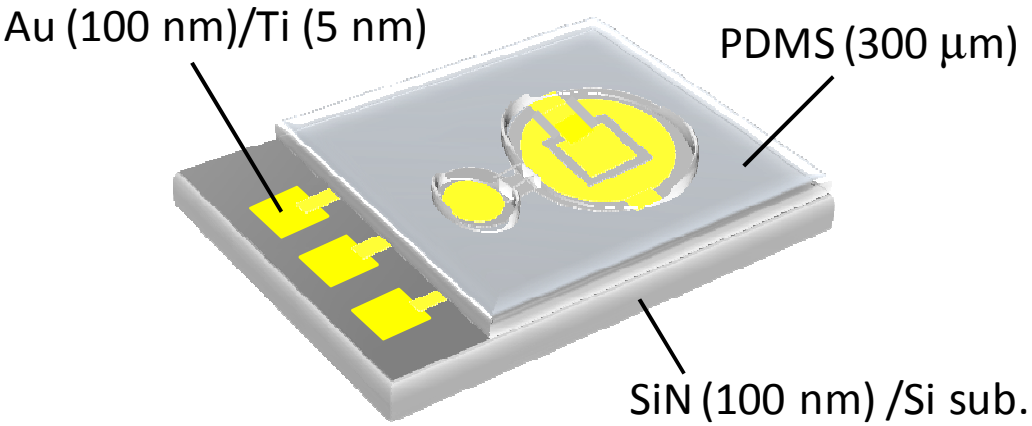
Au (100 nm)/Ti (5 nm)
PDMS (300 μm)
SiN (100 nm) /Si sub.

(b)

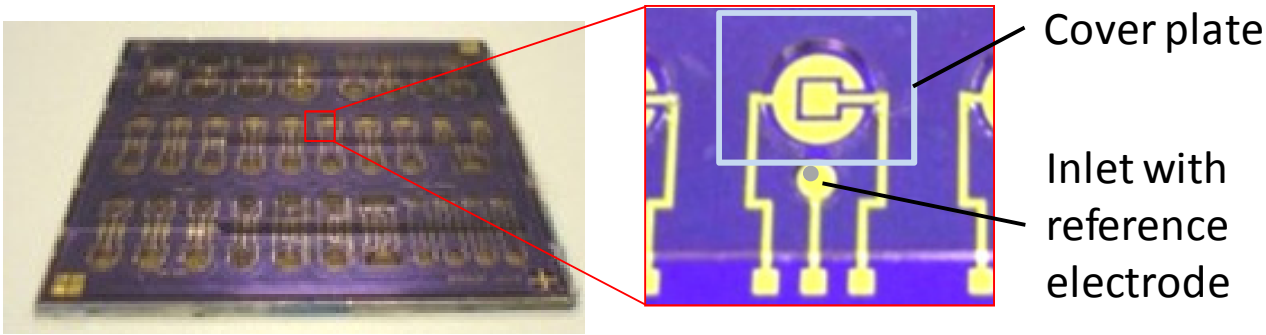
Cover plate
Inlet with reference electrode

Fig. 3

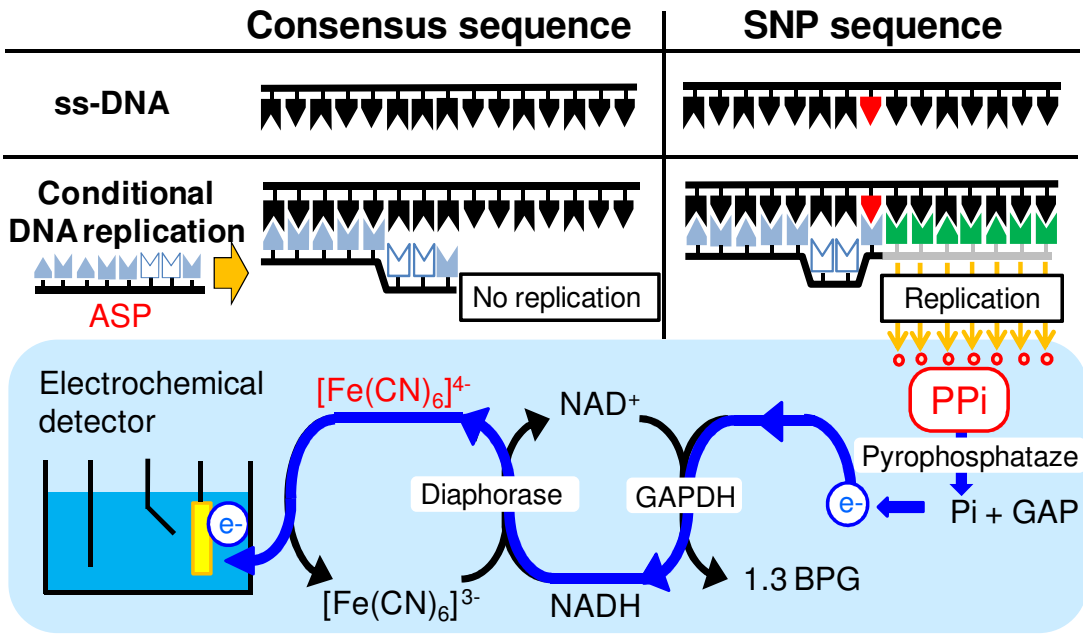
Consensus sequence
SNP sequence
ss-DNA
Conditional DNA replication
ASP
No replication
Replication
Electrochemical detector
[Fe(CN)6]4-
NAD+
PPi
Pyrophosphataze
Diaphorase
GAPDH
e-
Pi + GAP
1.3 BPG
[Fe(CN)6]3-
NADH

Fig. 4

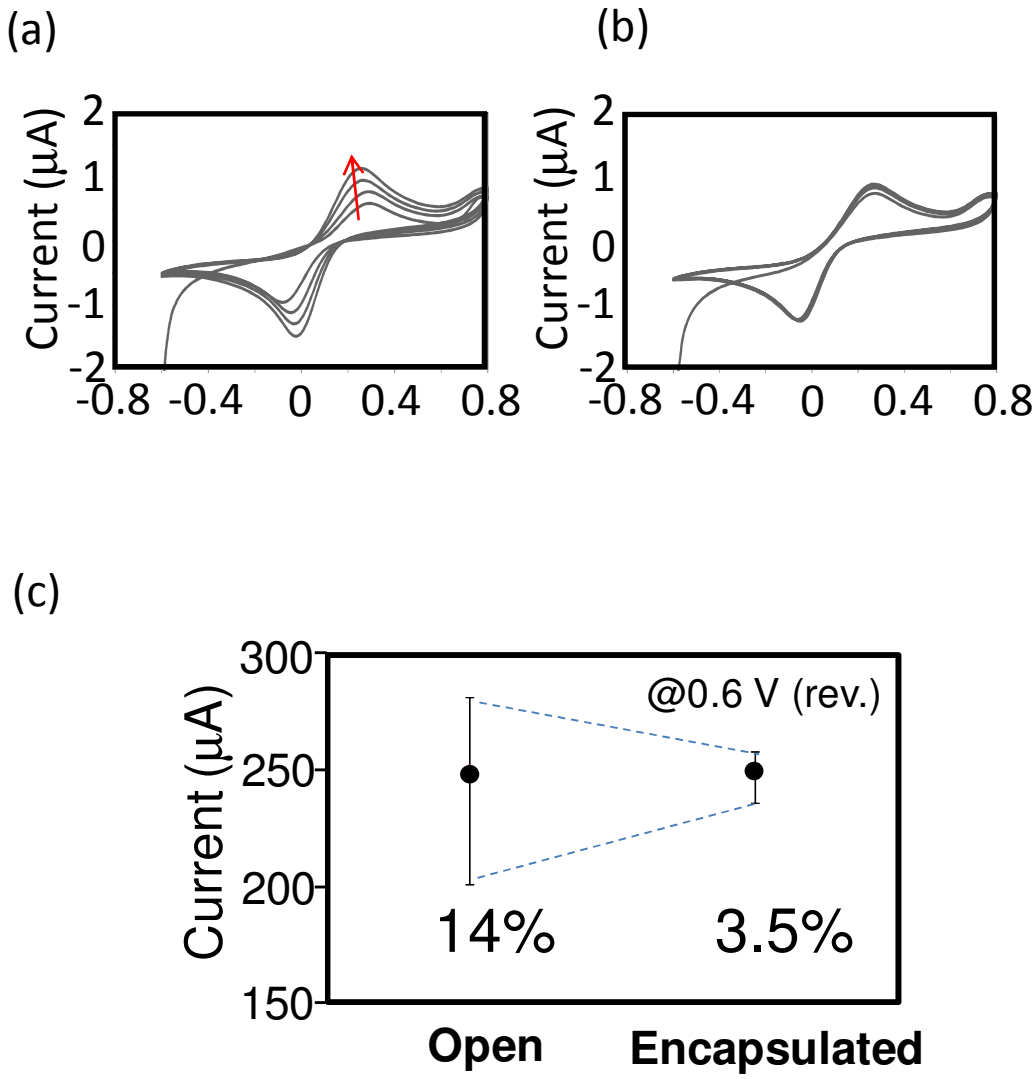
(a)
(b)
Current (μA)
2
1
0
-1
-2
-0.8
-0.4
0
0.4
0.8
(c)
300
250
200
150
@0.6 V (rev.)
14%
3.5%
Open
Encapsulated

Fig. 5

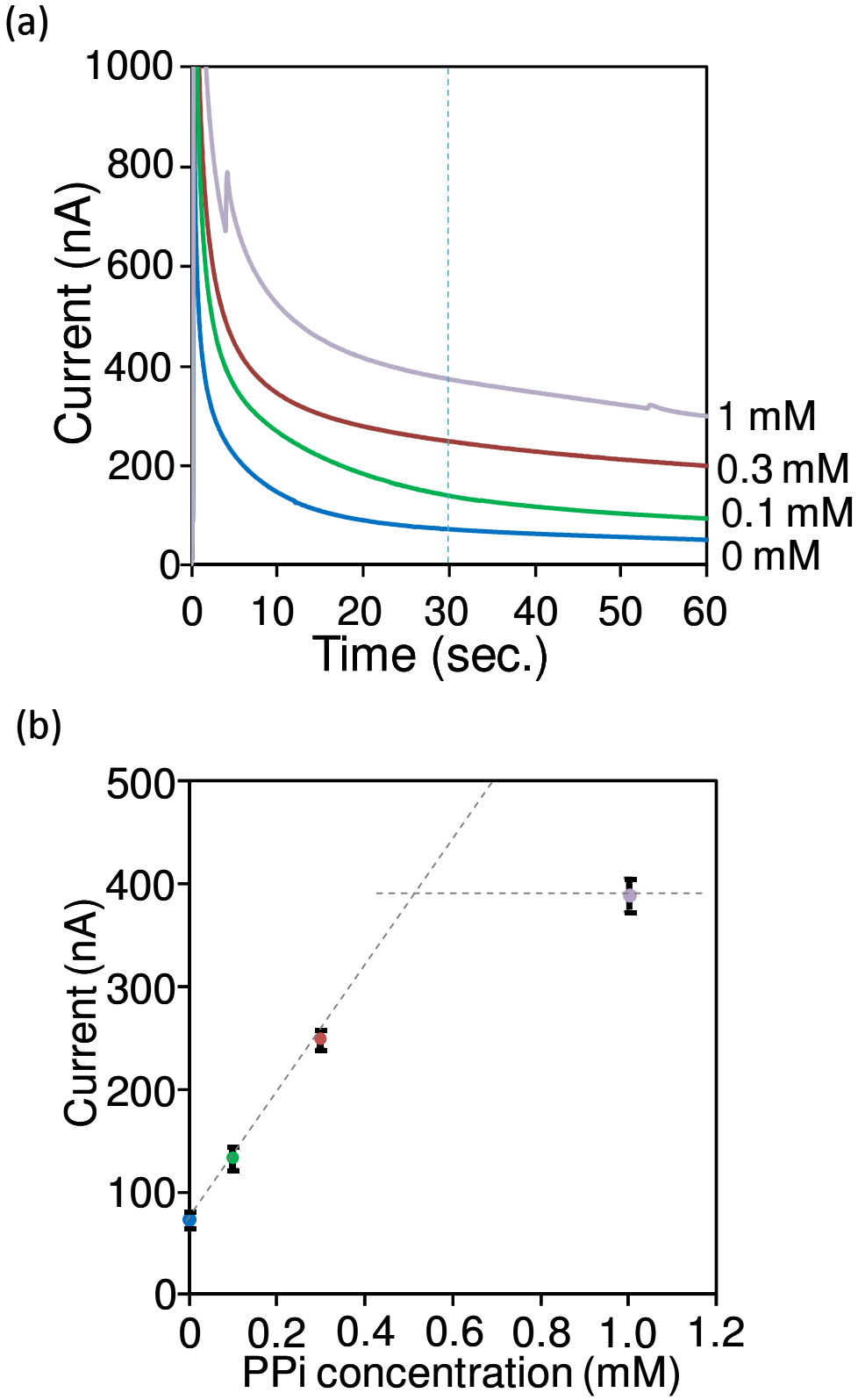
(a)
1000
800
600
400
200
0
Current (nA)
0
10
20
30
40
50
60
Time (sec.)
1 mM
0.3 mM
0.1 mM
0 mM
(b)
500
400
300
200
100
0
Current (nA)
0
0.2
0.4
0.6
0.8
1.0
1.2
PPi concentration (mM)

Fig. 6

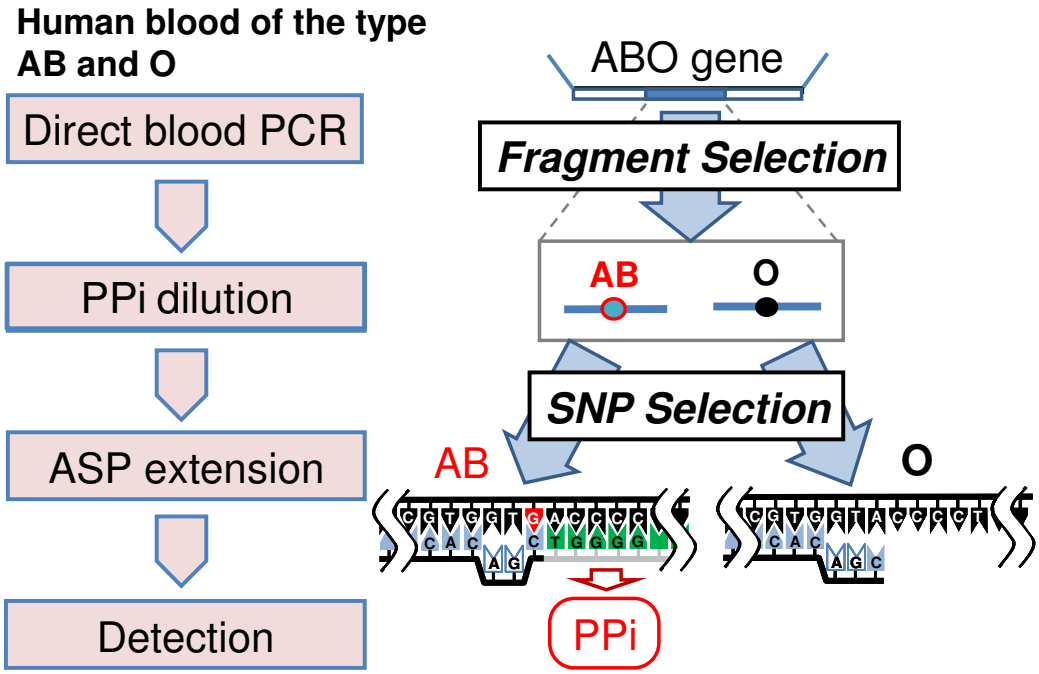
Human blood of the type AB and O
Direct blood PCR
PPi dilution
ASP extension
Detection
ABO gene
Fragment Selection
AB
O
SNP Selection
AB
O
PPi

Fig. 7

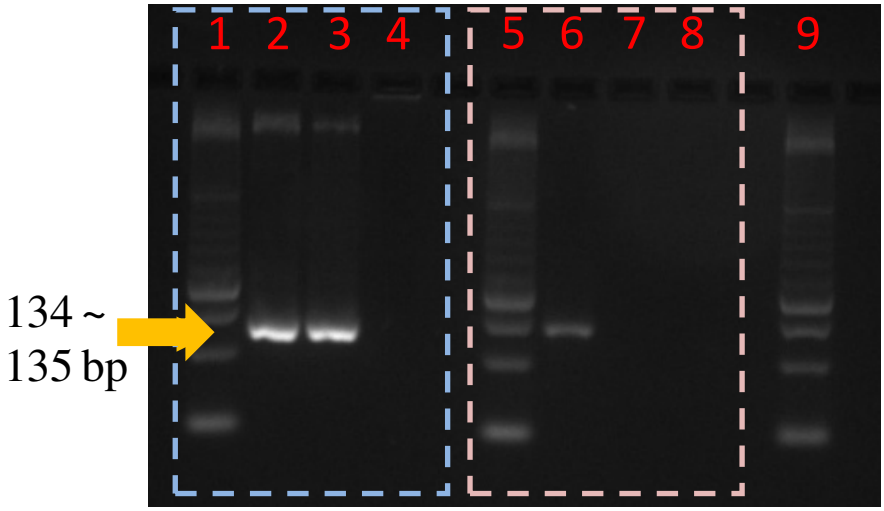

Fig. 8

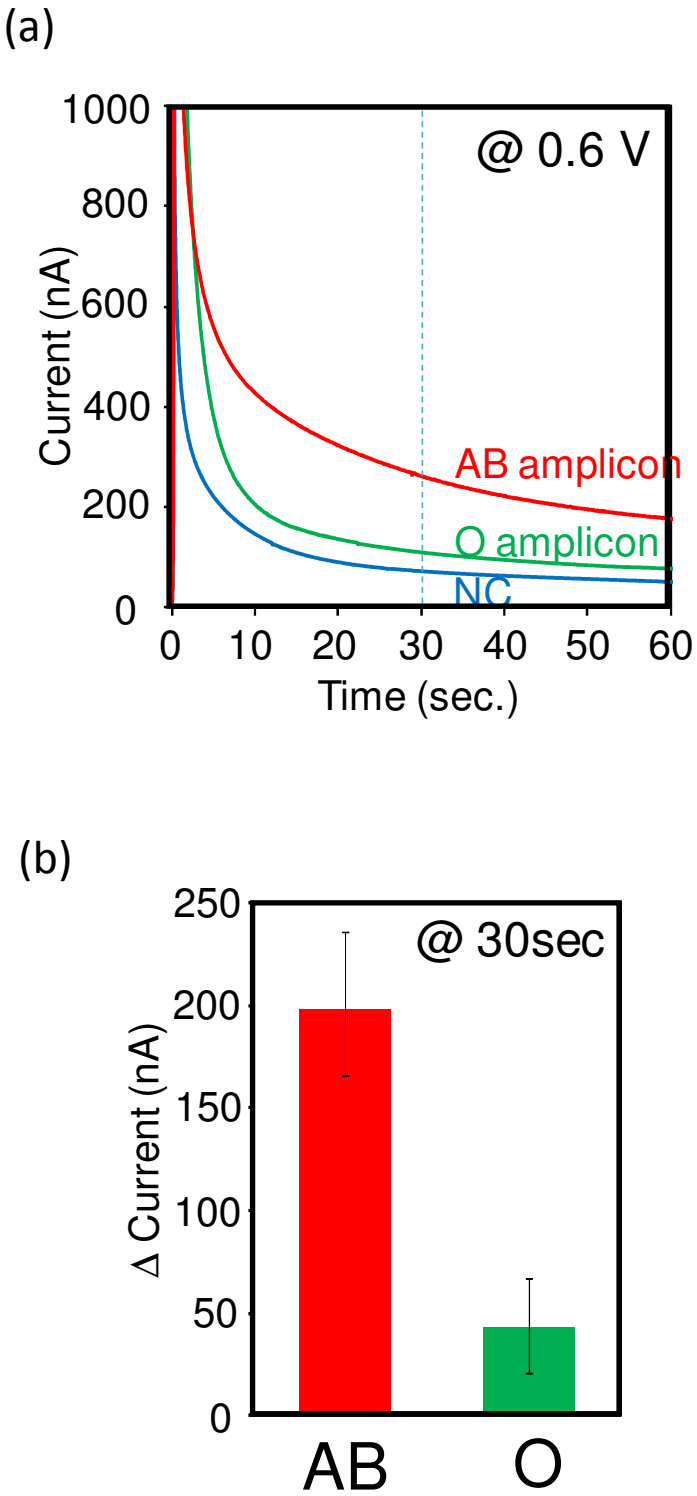
(a)
@ 0.6 V
Current (nA)
1000
800
600
400
200
0
0
10
20
30
40
50
60
Time (sec.)
AB amplicon
O amplicon
NC
(b)
@ 30sec
Δ Current (nA)
250
200
150
100
50
0
AB
O